Supporting Information

for

Adsorption and Diffusion of Small Alcohols in Zeolitic Imidazolate Frameworks ZIF-8 and ZIF-90

Jason A. Gee, Jaeyub Chung, Sankar Nair, and David S. Sholl*

School of Chemical & Biomolecular Engineering, Georgia Institute of Technology,

Atlanta, GA, 30332-0100

*Corresponding author: david.sholl@chbe.gatech.edu

Table of Contents

Experimental (Sim.) Structures

The coordinates for the experimental structures for ZIF-8 and ZIF-90 used in the simulations were obtained from the Cambridge Structural Database (CSD)[1]. The structure with the reference code (refcode) OFERUN was used for ZIF-8 and WOJGEI was used for ZIF-90. The ZIF-8 structure reported in the CSD was determined using neutron powder diffraction and has deuterium atoms substituted on the methyl groups, which were replaced with hydrogen atoms in our calculations. The simulation box used in all of the calculations consisted of 2 × 2 × 2 unit cells for each ZIF. The experimental and simulated lattice constants for each structure are reported in Table S22.

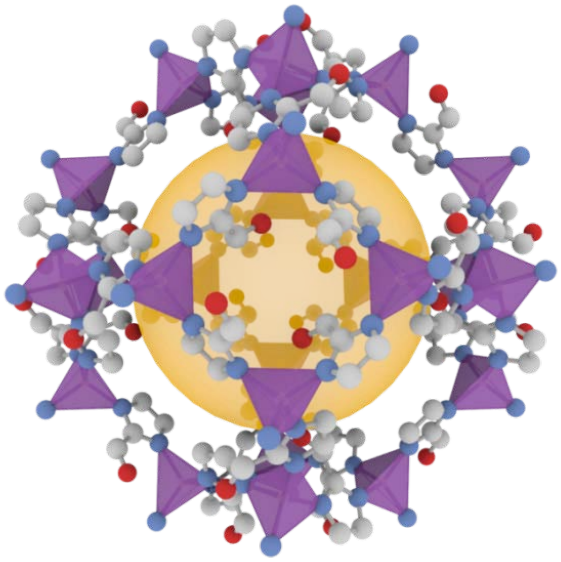

Figure S1. Schematic view of the ZIF-90 unit cell with the central yellow sphere representing the void volume of the framework. C atoms are grey, N atoms are blue, O atoms are red, and Zn atoms are purple. H atoms are omitted for clarity.

Force Field Parameters

The Lennard-Jones (LJ) parameters and charges for the alcohols were taken from the TraPPE[2] force field. The LJ parameters for the framework atoms were taken from the general AMBER (GAFF)[3,4] and DREIDING[5] force fields. Point charges were assigned to the framework atoms using density functional theory (DFT) calculations based on the DDEC method of Manz et al.[6,7] The bonded and non-bonded interaction parameters for the framework atoms of ZIF-90 (ZIF-8) are listed in Tables S1-S10 (S11-S20).

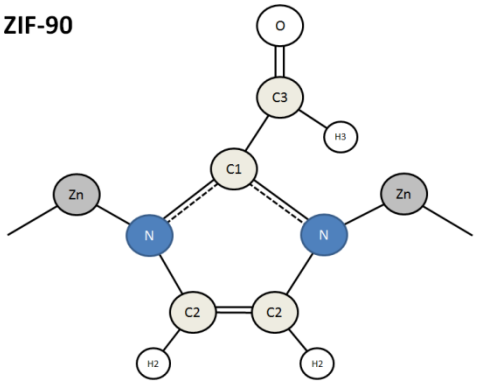

Figure S2. Schematic of the organic linker and metal center of ZIF-90 including the atomic symbols and numbering scheme used in the force field parameterization below.

GAFF/DREIDING Non-Bonded Interaction Potential (LJ+Coulomb):

Table S1. Lennard-Jones parameters and partial atomic charges computed using the DDEC method for framework atoms in ZIF90 from the GAFF force field.

#	Atom Type	ε (K)	σ (A)	q (e)
1	C1	43.3031	3.40	0.2104
2	C2	43.3031	3.40	-0.0001
3	C3	43.3031	3.40	0.2582
4	H2	7.5529	2.51	0.1149
5	H3	7.9053	2.65	0.0476
6	Zn	6.2941	1.96	0.6726
7	O	105.7402	2.96	-0.4091
8	N	85.5992	3.25	-0.3320

Table S2. Lennard-Jones parameters and partial atomic charges computed using the DDEC method for framework atoms in ZIF90 from the DREIDING force field.

#	Atom Type	ε (K)	σ (A)	q (e)
1	C1	47.8852	3.47	0.2104
2	C2	47.8852	3.47	-0.0001
3	C3	47.8852	3.47	0.2582
4	H2	7.6536	2.85	0.1149
5	H3	7.6536	2.85	0.0476
6	Zn	27.6939	4.05	0.6726
7	O	48.1873	3.03	-0.4091
8	N	38.9728	3.26	-0.3320

GAFF/DREIDING Bond Stretching Interaction Potential (Harmonic):

Table S3. Bond stretching interaction parameters in ZIF90 from GAFF.

#	Bond Type	k_b (kcal·mol^{-1}·A^{-2})	r_0 (Å)
1	C3-H3	340.00	1.09
2	C3-O	610.90	1.23
3	C1-C3	346.54	1.49
4	C1-N	488.00	1.335
5	Zn-N	78.50	2.011
6	C2-H2	367.00	1.08
7	C2-N	440.21	1.37
8	C2-C2	540.25	1.35

Table S4. Bond stretching interaction parameters in ZIF90 from DREIDING.

#	Bond Type	k_b (kcal·mol^{-1}·A^{-2})	r_0 (Å)
1	C3-H3	350.00	0.99
2	C3-O	350.00	1.22
3	C1-C3	350.00	1.33
4	C1-N	350.00	1.275
5	Zn-N	350.00	1.935
6	C2-H2	350.00	0.99
7	C2-N	350.00	1.275
8	C2-C2	350.00	1.33

GAFF Bond Bending Interaction Potential (Harmonic):

Table S5. Bond bending interaction parameters in ZIF90 from GAFF.

#	Angle Type	k_θ (kcal·mol^{-1}·rad^{-2})	θ_0 (°)
1	H3-C3-O	54.280	120.93
2	H3-C3-C1	46.357	116.20
3	O-C3-C1	68.299	123.58
4	C3-C1-N	66.015	123.92
5	C1-N-C2	71.254	105.27
6	N-C1-N	75.484	112.16
7	N-C2-C2	73.750	108.65
8	N-C2-H2	49.954	125.68
9	C2-C2-H2	49.451	125.67
10	Zn-N-C2	32.477	126.40
11	Zn-N-C1	48.680	128.33
12	N-Zn-N	35.240	109.48

DREIDING Bond Bending Interaction Potential (Cosine Harmonic):

Table S6. Bond bending interaction parameters in ZIF90 from DREIDING.

#	Angle Type	K_θ (kcal·mol^{-1}·rad^{-2})	θ_0 (°)
1	H3-C3-O	66.667	120.000
2	H3-C3-C1	66.667	120.000
3	O-C3-C1	66.667	120.000
4	C3-C1-N	66.667	120.000
5	C1-N-C2	66.667	120.000
6	N-C1-N	66.667	120.000
7	N-C2-C2	66.667	120.000
8	N-C2-H2	66.667	120.000
9	C2-C2-H2	66.667	120.000
10	Zn-N-C2	66.667	120.000
11	Zn-N-C1	66.667	120.000
12	N-Zn-N	56.250	109.471

.

GAFF Torsion Interaction Potential:

Table S7. Dihedral torsion interaction parameters in ZIF90 from GAFF.

#	Dihedral Type	k_ϕ (kcal·mol^{-1})	n	ϕ_0 (°)
1	X-N-C2-X	2.325	2	180.0
2	X-C2-C2-X	5.150	2	180.0
3	X-C1-N-X	5.000	2	180.0
4	X-C3-C1-X	2.325	2	180.0

Table S8. Improper torsion interaction parameters in ZIF90 from GAFF.

#	Improper Type	k_ϕ (kcal·mol^{-1})	n	ϕ_0 (°)
1	N-C3-C1-N	1.1	2	180.0
2	C2-H2-C2-N	1.1	2	180.0
3	C2-Zn-N-C1	1.1	2	180.0
4	N-C3-C1-N	1.1	2	180.0

DREIDING Torsion Interaction Potential(s):

Table S9. Dihedral torsion interaction parameters in ZIF90 from DREIDING.

#	Dihedral Type	K_ϕ (kcal·mol^{-1})	n	ϕ_0 (°)
1	X-N-C2-X	22.5	2	180.0
2	X-C2-C2-X	22.5	2	180.0
3	X-C1-N-X	22.5	2	180.0
4	X-C3-C1-X	22.5	2	180.0

Table S10. Improper torsion interaction parameters in ZIF90 from DREIDING.

#	Improper Type	k_ϕ (kcal·mol^{-1})
1	N-C3-C1-N	40.0
2	C2-H2-C2-N	40.0
3	C2-Zn-N-C1	40.0
4	N-C3-C1-N	40.0

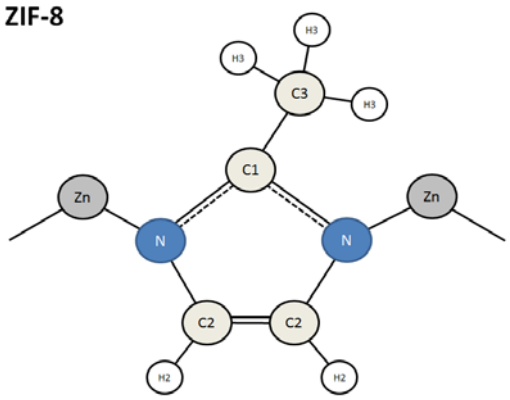

Figure S3. Schematic of the organic linker and metal center of ZIF-8 including the atomic symbols and numbering scheme used in the force field parameterization below.

GAFF/DREIDING Non-Bonded Interaction Potential (LJ+Coulomb):

Table S11. Lennard-Jones parameters and partial atomic charges computed using the DDEC method for framework atoms in ZIF8 from the GAFF force field.

#	Atom Type	ε (K)	σ (A)	q (e)
1	C1	43.3031	3.40	0.4375
2	C2	43.3031	3.40	-0.0662
3	C3	43.3031	3.40	-0.4606
4	H2	7.5529	2.51	0.1141
5	H3	7.9053	2.65	0.1381
6	Zn	6.2941	1.96	0.7072
7	N	85.5992	3.25	-0.4203

Table S12. Lennard-Jones parameters and partial atomic charges computed using the DDEC method for framework atoms in ZIF8 from the DREIDING force field.

#	Atom Type	ε (K)	σ (A)	q (e)
1	C1	47.8852	3.47	0.4375
2	C2	47.8852	3.47	-0.0662
3	C3	47.8852	3.47	-0.4606
4	H2	7.6536	2.85	0.1141
5	H3	7.6536	2.85	0.1381
6	Zn	27.6939	4.05	0.7072
7	N	38.9728	3.26	-0.4203

GAFF/DREIDING Bond Stretching Interaction Potential (Harmonic):

Table S13. Bond stretching interaction parameters in ZIF8 from GAFF.

#	Bond Type	k_b (kcal·mol^{-1}·A^{-2})	r_0 (Å)
1	C3-H3	340.00	1.09
2	C1-C3	346.54	1.49
3	C1-N	488.00	1.335
4	Zn-N	78.50	2.011
5	C2-H2	367.00	1.08
6	C2-N	440.21	1.37
7	C2-C2	540.25	1.35

Table S14. Bond stretching interaction parameters in ZIF8 from GAFF.

#	Bond Type	k_b (kcal·mol^{-1}·A^{-2})	r_0 (Å)
1	C3-H3	350.0	0.99
2	C1-C3	350.0	1.33
3	C1-N	350.0	1.275
4	Zn-N	350.0	1.935
5	C2-H2	350.0	0.99
6	C2-N	350.0	1.275
7	C2-C2	350.0	1.33

GAFF Bond Bending Interaction Potential (Harmonic):

Table S15. Bond bending interaction parameters in ZIF8 from GAFF.

#	Angle Type	k_θ (kcal·mol^{-1}·rad^{-2})	θ_0 (°)
1	C3-C1-N	66.015	123.92
2	C1-N-C2	71.254	105.27
3	N-C1-N	75.484	112.16
4	N-C2-C2	73.750	108.65
5	N-C2-H2	49.954	125.68
6	C2-C2-H2	49.451	125.67
7	Zn-N-C2	32.477	126.40
8	Zn-N-C1	48.680	128.33
9	N-Zn-N	35.240	109.48
10	C1-C3-H3	48.088	109.32
11	H3-C3-H3	35.000	109.50

DREIDING Bond Bending Interaction Potential (Cosine Harmonic):

Table S16. Bond bending interaction parameters in ZIF8 from DREIDING.

#	Angle Type	K_θ (kcal·mol^{-1}·rad^{-2})	θ_0 (°)
1	C3-C1-N	66.667	120.0
2	C1-N-C2	66.667	120.0
3	N-C1-N	66.667	120.0
4	N-C2-C2	66.667	120.0
5	N-C2-H2	66.667	120.0
6	C2-C2-H2	66.667	120.0
7	Zn-N-C2	66.667	120.0
8	Zn-N-C1	66.667	120.0
9	N-Zn-N	56.250	109.471
10	C1-C3-H3	66.667	120.0
11	H3-C3-H3	66.667	120.0

GAFF Torsion Interaction Potential:

Table S17. Dihedral torsion interaction parameters in ZIF8 from GAFF.

#	Dihedral Type	k_ϕ (kcal·mol^{-1})	n	ϕ_0 (°)
1	X-N-C2-X	2.325	2	180.0
2	X-C2-C2-X	5.150	2	180.0
3	X-C1-N-X	5.000	2	180.0

Table S18. Improper torsion interaction parameters in ZIF8 from GAFF.

#	Improper Type	k_ϕ (kcal·mol^{-1})	n	ϕ_0 (°)
1	N-C3-C1-N	1.1	2	180.0
2	C2-H2-C2-N	1.1	2	180.0
3	C2-Zn-N-C1	1.1	2	180.0

DREIDING Torsion Interaction Potential(s):

Table S19. Dihedral torsion interaction parameters in ZIF8 from DREIDING.

#	Dihedral Type	K_ϕ (kcal·mol^{-1})	n	ϕ_0 (°)
1	X-N-C2-X	22.5	2	180.0
2	X-C2-C2-X	22.5	2	180.0
3	X-C1-N-X	22.5	2	180.0

Table S20. Improper torsion interaction parameters in ZIF8 from DREIDING.

#	Improper Type	k_ϕ (kcal·mol^{-1})
1	X-N-C2-X	40.0
2	X-C2-C2-X	40.0
3	X-C1-N-X	40.0

Additional Simulation Details

Adsorbate molecules were inserted into the framework at a desired loading using the simple criterion that a move was accepted if it lowered the total energy of the adsorbate-framework system. The loadings used in the MD simulations were 4.5 mmol CH_3OH/g-ZIF and 2.25 mmol CH_3CH_2OH/g-ZIF. Molecular Dynamics (MD) simulations were performed in the NVT ensemble at T = 300 K using the LAMMPS simulation package[8]. After an energy minimization and 2 ns equilibration period, the MD production period consisted of 10 ns trajectories using many adsorbate molecules (~100 molecules CH_3OH/ simulation cell). During the MD production period, the coordinates of the center of mass of each adsorbate was collected and stored at each timestep and used to compute the mean squared displacement (MSD) using the built-in "compute MSD/molecule" command in LAMMPS. These values were averaged over the total number of adsorbates and then averaged over a period of 1 ps using the "fix ave/time" command and printed to an external file. The MSDs were then averaged over multiple time origins and trajectories to compute the self-diffusion coefficients using the Einstein relation[9]:

$$D_s = \frac{1}{6N} \lim_{t \to \infty} \frac{d}{dt} \left\langle \sum_{i=1}^{N} |r_i(t) - r_i(0)|^2 \right\rangle$$

where D_s is the self-diffusion coefficient, N is the number of adsorbate molecules, r is the position vector measured from the center of mass of each molecule, and the term in brackets denotes an ensemble average. An example of a plot of the MSD versus time used to compute the diffusivity is shown in Figure S4.

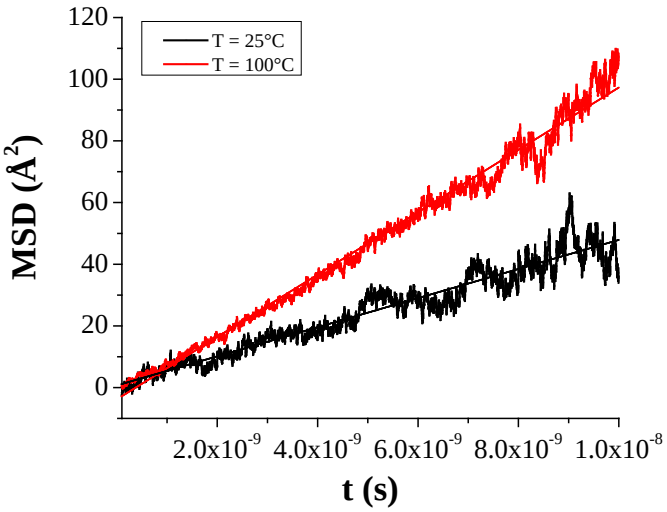

Figure S4. Average mean square displacement (MSD) plots for methanol in ZIF-90 at T = 25°C and T = 100°C during the MD production period using the GAFF force field including framework flexibility. The adsorbate loading used in these simulations was 14 molecules of CH_3OH /unit cell.

Figure S4 shows that in this example the average distance that the molecules travelled during the simulations, or root mean square displacement (RMSD), is smaller than the lattice constant of the material. In order to obtain physically accurate results in the calculation of the diffusion coefficient, the RMSD should typically be on the order of multiple unit cell lengths in order to ensure that a significant number of hops of the adsorbate molecules though the pores are observed during the course of the simulation. Due to timescale limitations it was not possible to obtain RMSDs of this magnitude in our simulations. We performed additional simulation runs to ensure that the simulation time did not have a significant effect on the diffusion coefficients calculated in our study, as described below.

To ensure the simulation time did not have a large effect on the values of the computed diffusivities, we ran additional simulations using a significantly longer MD production period. Here we used a timestep of 2 fs to decrease the overall CPU time needed for the simulations. We did not measure appreciable energy drift over the course of the simulation using this increased timestep. The simulation methods were the same as those described in the previous simulations but the MD production period in this case was 50 ns. The calculation of the MSDs here was similar to the method described in the previous section. The results from these simulations are shown in Table S21 and Figure S5. These results indicate that the diffusivity computed using the longer MD simulation runs are approximately within one standard deviation of the values reported for the shorter runs. Therefore, we assume that our original simulations have provided a sufficient number of inter-cage hops to provide a reasonable estimate of the molecular diffusivity in these systems.

Table S21. Diffusion coefficients for methanol in ZIF-90 at T = 25°C and T = 100°C using the GAFF force field including framework flexibility using an MD production period of 10 ns and 50 ns.

	$D_{s,\ CH3OH}$ ($\times 10^{-12}$ m^2/s)	
MD Production Period (ns)	T = 25°C	T = 100°C
10	6.3 ± 2.4	20.83 ± 2.6
50	6.7 ± 0.5	24.16 ± 0.3

Simulated and Experimental Lattice Constants

The lattice constants for ZIF-8 and ZIF-90 were simulated in the NPT ensemble using a production (equilibration) period of 1 ns (0.2 ns). The Nosé-Hoover thermostat (barostat) was used to control the temperature (pressure) with a decay period of 0.1 ps (1 ps). The results presented in Table S21 indicate that the GAFF force field more accurately predicts the experimental lattice constants of ZIF-8. These results for ZIF-8 are in good agreement with those reported by Zheng et al. [4] using GAFF.

Table S22. Lattice constants for ZIF-8 and ZIF-90 predicted using GAFF and DREIDING force fields.

ZIF	**L (Å)**		
	Expt.	GAFF	DREIDING
ZIF-8	16.99	16.74 ± 0.03	16.28 ± 0.02
ZIF-90	17.27	16.95 ± 0.02	16.49 ± 0.01

Simulated and Experimental Arrhenius Plots

The diffusion coefficients were determined for at least three temperatures for each component so that an Arrhenius relation could be used to find the activation energies for diffusion. The experimental and simulated Arrhenius plots are shown in Figure S5.

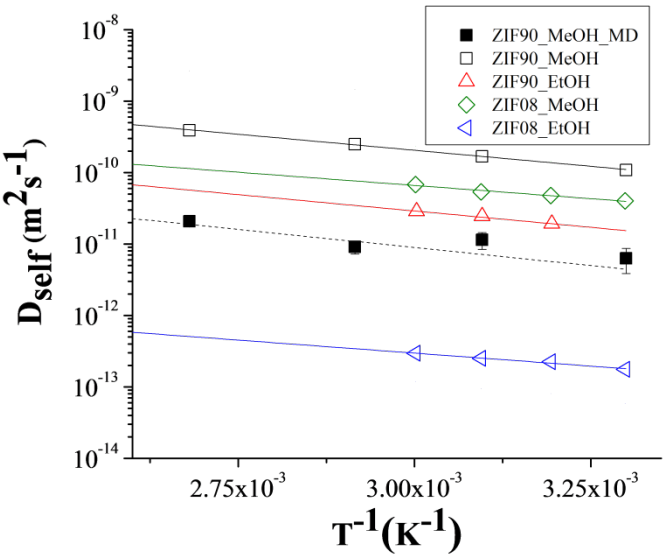

Figure S6. Self-diffusion coefficients for methanol and ethanol in ZIF-8 and ZIF-90 measured using PFG-NMR and simulated using MD over the temperature range T = 30-100°C plotted in Arrhenius form.

Supporting Information References

(1) Allen, F. *Acta Crystallographica Section B* **2002**, *58*, 380.

(2) Chen, B.; Potoff, J. J.; Siepmann, J. I. *The Journal of Physical Chemistry B* **2001**, *105*, 3093.

(3) Wang, J.; Wolf, R. M.; Caldwell, J. W.; Kollman, P. A.; Case, D. A. *Journal of Computational Chemistry* **2004**, *25*, 1157.

(4) Zheng, B.; Sant, M.; Demontis, P.; Suffritti, G. B. *The Journal of Physical Chemistry C* **2011**, *116*, 933.

(5) Mayo, S. L.; Olafson, B. D.; Goddard, W. A. *The Journal of Physical Chemistry* **1990**, *94*, 8897.

(6) Manz, T. A.; Sholl, D. S. *Journal of Chemical Theory and Computation* **2010**, *6*, 2455.

(7) Watanabe, T.; Manz, T. A.; Sholl, D. S. *The Journal of Physical Chemistry C* **2011**, *115*, 4824.

(8) Plimpton, S. *Journal of Computational Physics* **1995**, *117* (1), 1-19.

(9) Allen, M. P.; Tildesley, D. J. *Computer Simulation of Liquids*; Oxford University Press: New York, NY, 1987.